Suppression of V1 feedback produces a shift in the topographic representation of receptive fields of LGN cells by unmasking latent retinal drives

Jordi Aguila[1], F. Javier Cudeiro[1,2] and Casto Rivadulla[1]

[1] *Neurocom, School of Health Sciences and Centro de Investigacións Científicas Avanzadas (CICA), Institute of Biomedical Research (INIBIC), University of A Coruña, 15006 A Coruña, Spain and*
[2] *Cerebral Stimulation Center of Galicia, 15009 A Coruña, Spain*

Abstract

In awake monkeys, we used repetitive transcranial magnetic stimulation (rTMS) to focally inactivate visual cortex while measuring the responsiveness of parvocellular lateral geniculate nucleus (LGN) neurons. Effects were noted in 64/75 neurons, and could be divided into 2 main groups: (1) for 39 neurons, visual responsiveness decreased and visual latency increased without apparent shift in receptive field (RF) position and (2) a second group ($n = 25$, 33% of the recorded cells) whose excitability was not compromised, but whose RF position shifted an average of 4.5°. This change is related to the retinotopic correspondence observed between the recorded thalamic area and the affected cortical zone. The effect of inactivation for this group of neurons was compatible with silencing the original retinal drive and unmasking a second latent retinal drive onto the studied neuron. These results indicate novel and remarkable dynamics in thalamocortical circuitry that force us to reassess constraints on retinogeniculate transmission.

Introduction

Cortical feedback represents the most numerous input to the lateral geniculate nucleus (LGN), and from the classic work by Tsumoto et al. (1978), its influence on the physiology of LGN neurons has been broadly documented (for comprehensive reviews on the field, see references Wörgötter et al. 2002; Cudeiro and Sillito 2006; Sillito et al. 2006; Briggs and Usrey 2011). This evidence has shown a variety of effects exerted by the cortical feedback, including enhancement of the surround antagonism (Cudeiro and Sillito 1996), excitatory and inhibitory responses due to stimulation beyond classical receptive field (RF) (Marrocco et al. 1982), dynamic sharpening of the spatial focus (Jones et al. 2012), contribution to length tuning properties of LGN cells (Murphy and Sillito 1987), increasing the gain in a focal window at the thalamus (Rivadulla et al. 2002), introducing orientation discontinuity in the LGN (Sillito et al. 1993), gain control (Przybyszewski et al. 2000), or synchronization of relay cell firing and increased reliability and precision of spiking timing (Sillito et al. 1994; Wörgötter et al. 1998; Andolina et al. 2007). All these experiments have been carried out in anaesthetized animals, which could be masking some cortical influences as perceptual responses to sensory input critically depends upon brain state and, for instance, attention during alertness can affect our visual perception. In fact, when awake mammals have been studied, ranging from mice to nonhuman primates and humans, cortical feedback has been implicated in complex tasks, such as spatial attention, figure-ground modulation, or stimulus detection (Vanduffel 2000; O'Connor et al. 2002; McAlonan et al. 2008; Ortuño et al. 2014; Jones et al. 2015).

Cortical feedback has multiple opportunities for modulating LGN properties. Cortical afferents make excitatory contact on relay cells but also on γ-aminobutyric acid (GABA)ergic interneurons inside the nucleus and at the thalamic reticular nucleus (TRN) (Erisir et al. 1997; Van Horn et al. 2000). GABAergic neurons have an inhibitory effect on relay cells. The net balance appears to be excitatory as the cortical blockade tends to decrease thalamic activity, but subtle effects are visible with more spatially restricted cortical manipulation.

In the monkey, available data indicate that LGN neurons are essentially driven by one ganglion cell afferent (Lee et al. 1983; Kaplan and Shapley 1984; Sincich et al. 2007). These observations are consistent with Michael's (1988) study of the termination patterns of retinal axons in the LGN who stressed the restricted nature of the termination arrangement. The discrete retinopy characterizing retinogeniculate wiring seems echoed by the strong retinopy characterizing the cortical feedback (Cudeiro and Sillito 2006), meaning that the characteristic signature of any retinal image will in turn evoke a unique pattern of feedback from the visual cortex to the thalamus. This reflection of the influence of the cortical mechanism, therefore, would have the capacity to produce a selective retinotopic pattern of change in the thalamic mechanisms (Ichida and Casagrande 2002; Cudeiro and Sillito 2006; Andolina et al. 2013; Wang et al. 2016).

In this study, we investigate the influence of the feedback pathway from the striate cortex (V1) on the responses of LGN cells of behaving monkeys by decreasing cortical activity using low-frequency repetitive transcranial magnetic stimulation (rTMS). rTMS creates a magnetic field pulse that is highly focused and extremely short in time (less than 1 ms) and is able to modulate brain activity. It is well known that low-frequency repetitive stimulation (1 Hz and below) has an inhibitory effect on cerebral cortex activity. For instance, low-frequency rTMS usually results in suppression of corticospinal excitability. A 15 min train of 0.9 Hz at 115% resting motor threshold (RMT) applied over the primary motor cortex reduced corticospinal excitability for at least 15 min after the end of the stimulation (Chen et al. 1997; Muellbacher et al. 2000). It is also known that the duration of the effect is dose-dependent and, for example, a 4 min train of 1 Hz rTMS at 90% RMT reduced the motor evoked potential amplitude just for 2 min (Maeda et al. 2000). Similar effects have been shown in the visual system. For instance, 1 Hz rTMS applied to the cat visual cortex for 20 min significantly reduced early visual evoked potential amplitudes (Aydin-Abidin et al. 2006), and low rTMS (1 Hz, 30 min) applied to the visuo-parietal cortex of the cat induced a significant reduction of 14 C-2DG uptake in the stimulated cortex. High rTMS produced opposite effects. To reduce cortical input to LGN cells, we used an inhibitory rTMS protocol over the primary visual cortex (V1) that is known to induce the suppression of cortical activity: repetitive stimulation (intensity = 60% maximal output) for 4 min at low frequency (0.7 Hz) (Maccabee et al. 1990; Gangitano et al. 2002; De Labra et al. 2007; Ortuño et al. 2014).

Our data show unexpected and powerful effect on the LGN RF: focal cortical blockade shifted the field position by an average of >4°. We argue that such shifts under focal blockade silence the normal retinal drive and unmask latent retinal drives whose RF position lies beyond the retinotopic extent of our inactivation. These effects cannot be accounted for by our current understanding of retino-geniculo-cortical circuits and show the great capacity of cortical feedback to influence thalamic activity in awake states, demonstrating that RFs are dynamic structures regulated by the thalamo-cortico-thalamic interplay.
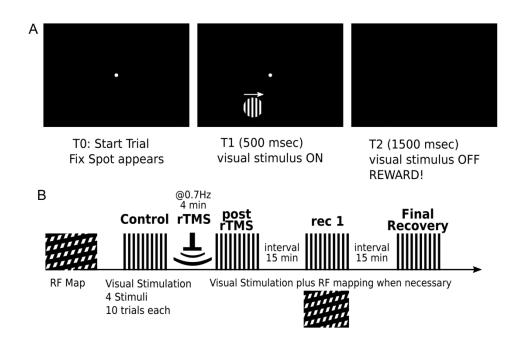
Materials and Methods

We recorded activity from 75 LGN parvocellular neurons from 2 awake male primates (*Macacamulatta*) following the rules of the Spanish Society of Physiology, the International Council for Laboratory Animal Science, and the European Union (Bylaw No. 86/809) and were approved by the ethics committee of the University of Coruña (Ortuño et al. 2014).

Visual Stimuli for LGN Recordings

We used a simple fixation task. Animals were trained using fluid reward, in conjunction with fluid control where necessary, to fixate a small spot (0.1°) presented on a video monitor placed at a distance of 57 cm from the animal. Animals had their head fixed, and their eye position was continuously monitored using an eye tracking system (iView; SR Research) recording at 250 Hz. After 500 ms of maintained fixation within a 0.5 ° window, the stimuli appeared on the monitor (1900 Belinea CRT monitor, 100 Hz refresh rate) for 1000 ms. The stimuli we used consisted of circular patches of 2 different diameters (0.6° and 6°) centered over the RF of the cell under test. Patches were filled with an achromatic sinusoidal grating (drifting or static) of 2 cycles/degree and were shown at a Michelson contrast of 0.6 and 2 Hz of temporal frequency (in the case of drifting gratings). The size of the stimuli was chosen to be sure that the RF center, in the case of small grating, and center plus surround, in the case of large grating, were fully covered. Visual stimulus presentation and control of the task were carried out using the Cortex software package (NIMH). Stimuli were presented on a gray background (17.9 cd/m^2), and monkeys had to maintain fixation during the task to receive a reward (a drop of juice or water). The trial was automatically aborted if fixation was broken at any time during the task.

To locate the RF position of the recorded cell, we presented visual stimuli covering each quadrant of the screen. The stimuli consisted of 16 luminance gratings with different orientations randomly presented at 15 Hz. In the quadrant where a visual response was obtained, we repeated the operation, dividing this region into 4 (and reducing the size of the grating accordingly), and so on, 6 times, allowing us to define the RF with a precision greater than 1 °.

The visual task (10 trials per stimulus) was performed in the control condition and immediately after rTMS over V1 (Fig. 1), ipsilateral to the recorded LGN. Biphasic pulses of rTMS were applied using a Magstim Rapid (Magstim Company Ltd, UK) with a figure-8 coil (25 mm inner coil radius) that generates a magnetic pulse of 1.5 T over the cortical surface (Deng et al. 2013). To obtain full recoveries, visual stimuli were presented 30 min after the end of rTMS and every subsequent 15 min until visual responses statistically similar to those obtained in the control were found (typically, responses were averaged over 10 stimulus presentations and were assessed from the accumulated count in the binned peristimulus time histograms (PSTHs) using separate epochs for baseline and visual responses). In those cases, where we did not find visual responses to smaller gratings after rTMS, the RF location was remapped, and the visual task was performed again.

(*A*) The trial starts with the fixation spot; 500 ms after fixation the visual stimulus is ON (stimulus duration 1000 ms). The animal must keep fixation until the stimulus disappear and then obtains the reward. If fixation is broken the trial is aborted. (*B*) Schematic representation of a standard recording session. Once a spike was isolated, the RF was mapped and then visual responses (4 different stimuli, 10 trials each) were obtained in control conditions. rTMS (0.7 Hz, 4 min) was applied over V1 ipsilateral to the LGN we recorded from. Visual responses were evaluated at different time intervals after rTMS. RF position was evaluated before each visual stimulation protocol and a complete RF mapping was made when necessary.

Extracellular Recordings

Extracellular single-unit recordings were made in the LGN using tungsten electrodes (FHC, Inc.) of 9–12 Mohm impedance. A recording chamber was centered 5.5 mm anterior to interaural 0 and 11.6 mm lateral to the midline. Dura mater was maintained intact during the experiment, and a guide tube was used to place the electrode into the brain; the guide tube remained well above the LGN. LGN recordings were verified by the nature of the visual response and the alternation of the ocular input of the responses as the electrode progressed through the LGN layers. LGN cells were recorded at eccentricities ranging from 1 to 18° (mean: 8.091 ± 4.289°).

Data Analysis

Spike waveforms from each neuron were sampled at 25 kHz, filtered between 250 and 8 kHz, and collected with a Spike2 System (Cambridge Electronic Design, UK). Offline analyses were carried out using custom Spike2 (CED, UK) and Matlab R2015a (Mathworks, Inc.) scripts. Recordings were sorted offline using principal component analysis (PCA). To ensure that the recorded cell waveform was the same during the full protocol, spikes were analyzed using a gamma-index analysis (GIA) (Low et al. 1998). GIA was performed by measuring the acceptability as the multidimensional distance between the data points of 2 spike waveforms in both the voltage and time values, scaled as a fraction of the acceptance criteria. In a space composed of voltage and time coordinates, the acceptance criteria create an ellipsoid surface (tolerance ellipse):

$$1 = \sqrt{\frac{r^2}{\Delta D^2{}_m} + \frac{\delta^2}{\Delta \delta^2{}_m}},$$

where $r2$ is the difference between points on the x-axis (time difference) and $\delta2$ is the difference on the y-axis (voltage difference). $\Delta D2m$ and $\Delta d2m$ are the time and voltage tolerance values, respectively: 3% of a voltage point for the voltage-axis and 0.025 ms for the time-axis. The axis scales are determined by individual acceptance criteria, and the center is located at the comparison data point. The minimum radial distance between both waveform points is termed the γ-index, so if $\gamma < 1$, then the comparison passes the test. If more than 85% of the points have a gamma index below one, then GIA passes the acceptance test, so we are comparing the same waveform profiles. All recorded cells passed the GIA.

Repeated presentations of the same stimuli were used to generate PSTHs. A PSTH provides a means of correlating the discharges of neurons with the stimuli onset. These histograms were made using the optimal bin size following the *Freedman–Diaconis Theorem* (Freedman and Diaconis 1981), which provides the optimal number of bins calculated by the expression:

$$\# of\ bins = 2[Q_3 - Q_1]n^{-1/3}\ ,$$

where $[Q3{-}Q1]$ is the interquartile range of the data, and n is the number of observations in the sample.

Phase-shifts were measured by fitting PSTHs using a sinusoidal equation:

$$y(t) = a * \sin(b * t + c) + d,$$

where a, b, c, and d are fit parameters. Phase difference was calculated by the absolute value of the difference between sinusoidal arguments:

$$\Delta_\varphi = |[b * t + c]_{control} - [b * t + c]_{new\ RF\ location}|.$$

Statistically, the data were analyzed with a 3-way analysis of variance for repeated measures (ANOVA-RM), performing the Greenhouse–Greiser correction for nonsphericity when necessary. Three within-subjects factors were set, the factor CONDITION with 3 levels (Control, rTMS, and Recovery), the factor SUBJECT with 2 levels (monkey A and monkey B) and the factor STIMULUS with 4 levels. In the case of significant differences, post hoc analysis was performed using the Tukey HSD test (Honestly Significantly Different). Results were considered significant when $P < 0.05$.
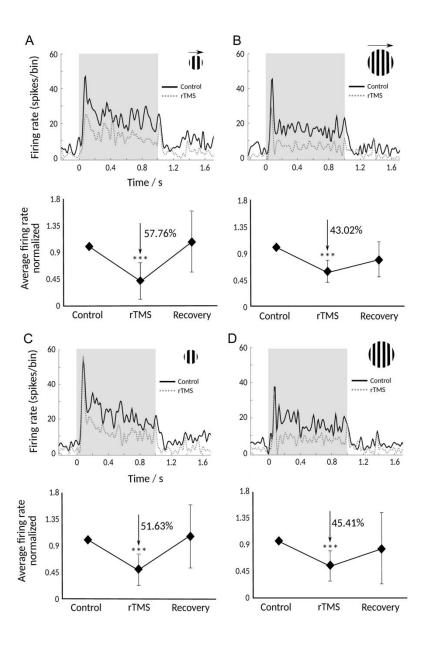
Results

We recorded 75 LGN cells from 2 awake behaving monkeys during spontaneous and visual guided activity: Monkey#1, 50 cells from the right LGN, plus 10 cells from the left one; Monkey#2, 15 cells from the right LGN. Physiological response properties, electrode depth and stereotypical shifts in eye preference were compatible with recordings obtained from parvocellular layers. To explore the effect of the cortical feedback on LGN responses, we used simple visual stimuli (as employed in the classical experiments with anaesthetized animals). The stimulation consisted of the presentation of 2 sets of stimuli: static gratings, temporally modulated, considered to drive LGN neurons strongly but not to activate corticothalamic cells very well, and drifting gratings, spatiotemporally modulated, which should be more effective at driving cortical neurons. Two different sizes of gratings were used: One adjusted to cover only the RF center and the other including center plus surround.

Our results can be divided into 3 groups: Cells whose RF position was modified after rTMS to V1 (33% of the whole sample, 25 cells; see below), cells whose firing rate was reduced but RF position was not modified (39 out of 75, 52%) and those not affected by our protocol (11 out of 75, 15%).
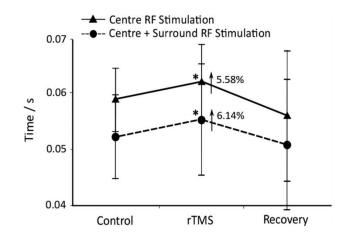
Group 1: Cortical Blockade Reduces LGN Cell Responsiveness

For those cells that did not shift the RF position ($n = 50$), the most common effect observed (39 out of 50 cells, 34 in monkey#1 and 5 in monkey#2) after low-frequency rTMS application to V1 was a reduction of visual responses ($P < 0.001$, ANOVA with Repeated Measures; ANOVA-RM). The PSTHs shown in Figure 2 illustrate these findings. rTMS produced a decrease in the response to all stimuli (A–D) for an individual cell (top panels) and for the averaged population. There was a tendency for a higher decrease in the responses evoked by the small drifting grating, but these differences were not statistically significant ($P > 0.05$, ANOVA-RM). Additionally, there was a significant reduction in spontaneous activity after rTMS ($11.64 \pm 1.02\%$, $P < 0.01$ ANOVA-RM).

Visually evoked responses obtained with the 4 stimuli employed in the different experimental situations. (*A*) Small drifting grating, (*B*) Large drifting grating, (*C*) Small static grating, and (*D*) Large static grating. In each of the panels, a representative cell (top) and the population data averaged across the whole stimuli and normalized (bottom) are shown. Recovery data were recorded 30 min after rTMS. (***) $P < 0.001$.
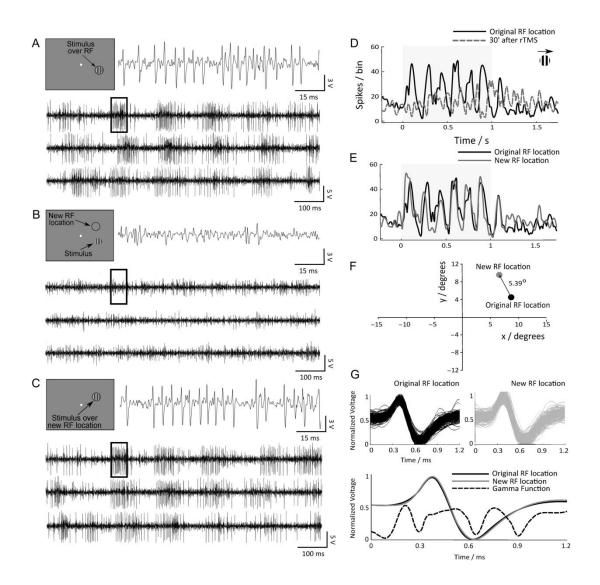
Interestingly, after applying rTMS the reduction in firing rate was accompanied by an increase in peak latency, defined as the time from the stimulus appearance to the maximum response. The latency was calculated and averaged only for the static stimulus as drifting grating could introduce variability in the responses due to trial by trial variations between the stimulus phase, the start of the movement and the RF position. After cortical blockade, there was a significant increase ($P < 0.05$, ANOVA-RM) for both small and large gratings of 5.58% (3 ms) and 6.14% (3.3 ms), respectively (Fig. 3). There were not specific differences related to the stimulus size ($P > 0.05$, ANOVA-RM).
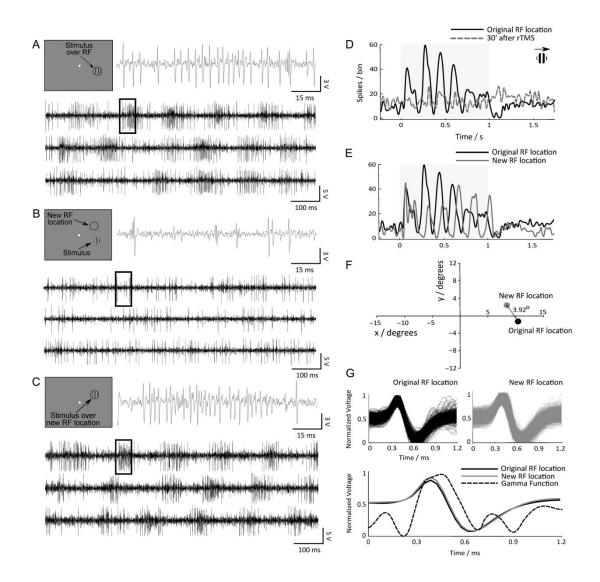

Averaged latency for those cells that decreased firing rate after TMS in V1 ($n = 39$) obtained with center stimulation alone (continuous line) and center+surround (dashed line) stimulation in different experimental conditions. (*) $P < 0.05$.

Group 2: Cortical Blockade Shifts RF Position

Twenty-five cells (33% of the recorded sample, 16 in monkey#1 and 9 in monkey#2) showed a displacement in RF position after rTMS to V1. Figures 4 and 5 show raw records from 2 different LGN neurons under visual stimulation with a 0.6 ° drifting grating over the RF before (*A*) and after rTMS (*B*). After rTMS application, the neural response obtained during control was silenced, and the stimulus was not able to evoke visual response. When the RF was remapped, a new location for the cell was found, and it was located 5.39 ° apart from the original position in the case of the cell illustrated in Figure 4 and 3.92 ° for the cell shown in Figure 5. Again, a visual response was obtained (*C*). The insets at the upper left corner of each panel graphically represent (not to scale) the position of the stimulus for each condition. It is very clear that after TMS, there was a shift in the RF location.
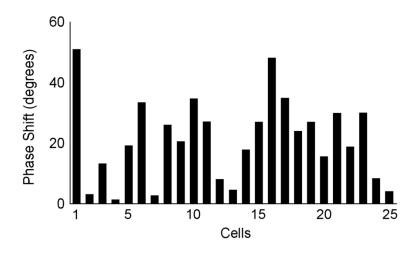
Visual responses (raw traces) recorded from one single cell when the visual stimulus (small drifting grating) was centered on the RF initial location in control (*A*), after rTMS (*B*), and in the new RF location (*C*). The RF position is schematically depicted in the insets. Three trials are shown for each stimulation position, and the area inside the square is expanded (upper trace in each case). (*D*) PSTHs representing the averaged response (10 trials) obtained from the same neuron in control (continuous black line) and 30 min after rTMS (dashed gray line). (*E*) PSTHs comparing the original response (black, same as in D) with the one obtained 30 min after rTMS once the RF was remapped and the visual stimulus was placed in the new location (gray line). Visual stimulus was a 0.6 ° diameter drifting grating, and the gray area represents stimulus duration. The displacement of the RF center was 5.39 ° in this particular example (*F*). The mean shift was 4.53 °. (*G*) All spikes obtained with visual stimulation at the original RF position for the same cell in control (top left) and at the new RF position after rTMS (top right). For each experimental session, we analyzed spike waveforms with a GIA (see Materials and Methods). We compared the average value of spikes recorded at the original and new (displaced) RF location, obtaining a gamma function as the output (bottom). If more than 15% of the points of the gamma function have a value above one, then the test fails, and we cannot ensure that the waveforms are the same. The results demonstrate that we were recording the same cell. Only those cells that passed the test were included in the study.

Another example obtained from a different neuron (see legend for Fig. 4). Notice in this case the phase displacement in the visual response at the new location.

The PSTHs in *D* are the averaged responses to the same grating when presented prior to rTMS (black) and after rTMS (gray). Visual stimulation over the "new RF" (*E*) induced a response very similar to the original (gray line). The *X/Y* chart shown in *F* represents the original and new positions of the RF for the cell. On average, for the 25 cells there was not significant decrease in visual activity at the new position, however, spontaneous activity was reduced by 24.04% ± 13.80 (*P*< 0.05 *t*-test). In Figure 4, phase of the response did not shift between the 2 locations (3.24°). However, in Figure 5 the phase-shift was considerable (50.4 °). As we will argue, RF position shift imposed by rTMS is attributable to loss of retinal ganglion cell drive and unmasking of a second retinal ganglion cell whose RF is outside the topographic bounds of area 17 blockade. The shift in phase is consistent with this idea as there is no reason for the second retinal ganglion drive to possess the identical phase relationship. This is reinforced by the fact that the other group of cells (group 1, see above) showed no phase-shift (0.16 ° in average). Figure 6 shows the observed phase-shifts among the 25 LGN neurons that showed shifts in RF position. The phase-shifts appeared random, and there was no correlation between the magnitude of phase-shift and the size of RF displacement (Pearson index *r* = 0.0624).

Phase displacement in visual responses in the new RF location. The graph shows the phase changes for each of the 25 cells that experienced variations in the position of their RFs after TMS.

The average displacement obtained for the whole population was 4.53 ± 1.95°. The displacement of the RF central location was calculated by the definition of Euclidian distance:
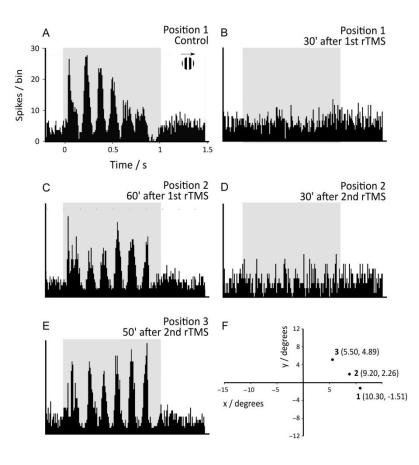
$$d = \sqrt{(x_1 - x_0)^2 + (y_1 - y_0)^2},$$

where (x0,y0) and (x1,y1) are the original and new RF locations, respectively. This value could be an overestimation of the actual displacement as smaller shifts were probably not detected (see discussion below).

To be sure that we were recording the same cell throughout the recording session, we performed a gamma-index test for every recorded neuron (see Materials and Methods), comparing the spike waveform in the control and after rTMS; those cells that did not pass the test were discarded from the study. Figures 4 and 5G show the spike waveform in the control (left) and after rTMS when the visual stimulus was placed on the new RF location (right). The comparison between the averaged waveforms recorded in both situations (superimposed) plus the result of the GIA for this cell are depicted in the bottom panel. All of the points have a gamma index that is lower than 1, so we determined that both waveforms correspond to the same cell. New RF position tended to exhibit longer visual latencies, but the difference was not significant (0.0601 ± 0.0056 sec in control, versus 0.0636 ± 0.0062 after rTMS ($P > 0.05$) Supplementary Fig 1.).

As a complementary analysis, when a shift in the RF of individual neurons was observed, we also compared the multiunit activity recorded at that location before and after rTMS. In all cases, a similar displacement in the visual space of the locus of activity was detected (see Supplementary Fig 2.). It seems that rTMS produced a scotoma-like effect affecting the neurons at the recording place.
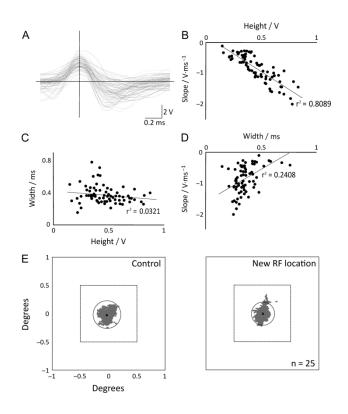
In 3 of the neurons whose RF was displaced after magnetic stimulation, it was possible to apply rTMS more than once after the RF was remapped. Figure 7 illustrates the results of one cell at different times after rTMS. After a second block of rTMS, the RF position shifted even more compared with the original situation but maintained the displacement direction. Interestingly, the first RF displacement resulted in a phase-shift in the response by 30.13 °, and the second RF displacement yielded a different phase-shift of 13.08 ° from the first displacement. Such dynamic shifts in phase and spatial position would be consistent with silencing the first retinal drive, unmasking a second (latent) retinal drive with the first rTMS block, and then silencing the second (latent) retinal drive and unmasking a third (latent) retinal drive with the second rTMS block.

Single cell responses after 2 consecutive blocks of rTMS application. *A* and *B* illustrate the response of the cell in the original RF position in control and 30 min after the first block of rTMS. (*C*) Response of the neuron in the new location (position 2) after careful remapping of the RF. (*D*) Illustrates the response at this same position shown in (*C*) but after the end of the second block of rTMS. (*E*) Cell response after RF was remapped again, as the visual stimulus was centered in the new location (position 3). (*F*) Map of coordinates depicting RF positions at the beginning of the experimental protocol and, consecutively, after different blocks of rTMS. RF shift was 3.7 ° after the first rTMS block and 4.5° after the second.

Once the RF displacement was detected, we always attempted to obtain a recovery of the initial situation (e.g., RF shift to the original position). After recovery times of up to 3 h, it never happened. It is worth mentioning that in several occasions, we have used the same coordinates for next day penetration. In all cases, the position of the RF was similar to the one at the beginning of the recording session of the previous day, suggesting that the scotoma-like effect had disappeared.

These results would indicate that cells located in a particular area seem to be affected similarly regardless of cell type, but the possibility still exists that neurons that shift (a third of the recorded cells) might belong to a particular subset of neurons, such as interneurons. To minimize this possibility, we performed a series of analysis. A PCA for every average waveform of the sample (Fig. 8*A*), including height, width at half-high, and slope. The Pearson product-moment correlation coefficient showed a linear correlation between height and slope ($r2=0.8089$) (Fig. 8*B*), while the width did not show any correlation with the other 2 variables ($r2 \leq 0.25$) (Fig. 8*C,D*). The width at half-high is an independent variable characteristic of the cell under test, so we performed a histogram of this variable with a bin width of 0.045 ms (using the Freedman–Diaconis theorem, see Materials and Methods). This analysis reveals just one averaged width of 0.36 ± 0.02 ms. Hence, according to the parameters included in the analysis, we failed to detect differences that could be attributed to cell type. Specifically, we could not find evidence that those cells may be interneurons, whose spikes are known to be narrower than those of relay cells, as they have a faster repolarization (Pape and McCormick 1995). For these group of cells we also checked ocular movement dispersion during fixation (Fig. 8*E*), reasoning that if TMS produced an alteration in ocular movements coordination (temporary strabismus) this would be expressed during the fixation periods. We did not find differences before and after the RF shift ($P > 0.05$).
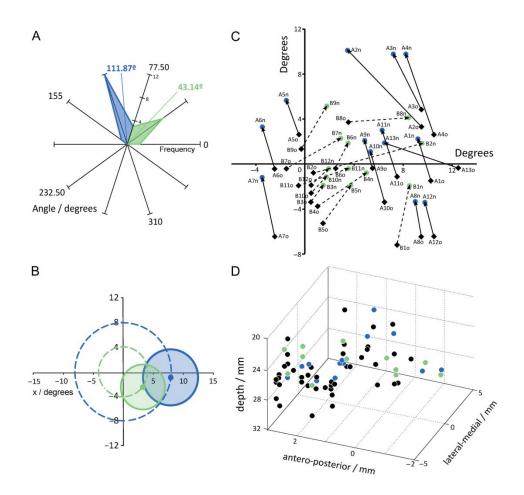
PCA was performed for all spike waveforms recorded (*A*). Pearson product-moment correlation coefficients reveal linear correlations between height and slope (*B*), while the width did not show any correlation with the other 2 variables (*C,D*). Example of ocular movement dispersion during fixation before and after TMS for those cells with RF shift. The circle shows the bidimensional standard deviation centered at the mean value for the points. ($P > 0.05$ *t*-test) (*E*).

To know if different modes of thalamic activity (burst or tonic, see Sherman 2001) could account for the observed effects, the percentage of spikes in burst mode in each group was analyzed. A burst was defined as a minimum of 2 or more spikes with an interspike interval (ISI) of less than 4 ms, and with the cardinal spike following a quiescent period of at least 50 ms. Such patterns are thought to represent the extracellular signature of the activation of an underlying calcium current, the basis for the burst mode (Lu et al. 1992) which can occur in wakefulness (Guido and Weyand 1995). Both groups are almost identical, percentage of spikes in burst was 7.1 in those cells that did not jump, versus 7.8 for those that did, similar to previously reported in similar conditions (Ramcharan et al. 2003; Ortuño et al. 2014). Finally, we performed an ISI analysis that could detect some differences on the cell properties. Supplementary Figure 3 shows the results of these analyses for each visual stimulus. Again, there were no evidence for support that cells in the 2 groups belong to different cell groups.

We analyzed the direction for the RF displacement, and we found 2 principal angular directions for the shifts: $\vartheta_1 = (111.87 \pm 16.43)°$

(subgroup A) and $\vartheta_2 = (43.14 \pm 22.66)°$ (subgroup B) (see Fig. 9*A*). We studied both subgroups, and we found significant differences in their RF eccentricities ($P < 0.05$, *t*-test) (Fig. 9*B*), obtaining an average eccentricity of $(8.51 \pm 4.55)°$ for subgroup A and $(4.88 \pm 3.54)°$ for subgroup B. Figure 9*C* shows the original and the new RF position, after TMS for each cell. Moreover, when the same analysis was performed to compare the group of neurons whose RF position did not change compared with those who did, the eccentricity of cells whose RFs were displaced after cortical blockade $(6.85 \pm 3.95)°$ was significantly less ($P < 0.01$, *t*-test) than that of the other cells $(10.08 \pm 4.35)°$ (Fig. 9*B*). Checking for possible unintentional bias during the recordings, we made a reconstruction of the recording position for each cell (Fig. 9*D*), no differences were found between both groups.

(A) Polar plot representing the RF shift direction. It is clear that there were 2 main angular directions for the displacement: 111.87 (blue) and 43.14 ° (green). (B) Mean RF position of both subgroups and the bidimensional standard deviation. Dashed line shows the eccentricity of the RFs for each subgroup. (C) Representation of RF initial and final positions for cells whose RF shifted during TMS (n = 25). Displacement toward 111 °, continuous line; displacement towards 43 °, dashed line. (D) Schematic representation of the recording position for each recorded cell (n = 75). There is no obvious pattern of spatial distribution.

Discussion

rTMS Modifies Retinotopic Organization of LGN

rTMS stimulation that should have focally depressed corticogeniculate activity altered retinopy in at least one-third of the LGN neurons. Such alteration is unprecedented and not supported by what we understand about retinogeniculate organization in the monkey. The shifts in RF position were sizeable, averaging 4.5 °. Because retinal input is necessary for LGN activity such shifts force us to explain 2 phenomena: focal inactivation silences a retinal drive and focal inactivation unleashes one or more latent retinal drives.

It is not easy to account for the circuits unleashed here, especially the shift in RF position, as we have to account for 2 phenomena that have never been observed: silencing of the original drive and initiating activity in a latent retinal drive. Silencing the retinal drive could occur if we assume that loss of discrete circuits from cortex were somehow necessary for maintaining retinogeniculate transmission. The shift in RF position would posit the existence of latent retinal drives to the LGN neuron that are unmasked because of loss of focal cortical downflow. These new drives become functional as their cortical influence must be coming from cortical regions beyond the block. This seems to be supported by the fact that 72% of the affected neurons respond to visual stimulation at the new RF location with a shift of phase greater than 10 °. Such speculation would also be consistent with those LGN neurons whose RF did not shift, but whose responsiveness was compromised. This

would be because their circuits are compromised, but not enough to silence the retinal drive, and the complete absence of a phase-shift would suggest that the original retinal drive is still intact.
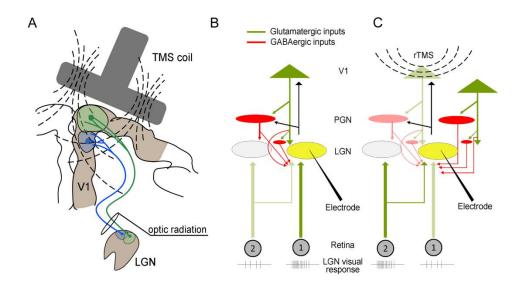
To interpret our findings, it would have been useful to simultaneously record from V1 neurons during rTMS application as the observed phenomenon could be related to a topographic reorganization of the primary visual cortex after rTMS. Unfortunately, at least in our hands, recordings under these circumstances (awake animal) for the long period needed, and at the same place were TMS has to be applied, were not technically possible.

Even if we admit that small shifts (less than 1 °) could be classified as "not displaced RF" hence underestimating the percentage of "displaced" cells and, consequently, overestimating the average displacement; the magnitude of the RF shifts we observed is unprecedented; far greater than observed in anesthetized cats, below 0.5 ° (Espinosa et al. 2011; Wang et al. 2016). In the sensory system, there exists an organized topographic map of the sensory inputs (retinotopy, somatotopy, etc.) (Kaas 1997). These maps, far from being immutable, exhibit a high degree of plasticity (Gilbert and Wiesel 1992; Darian-Smith and Gilbert 1995; Gilbert 1998; Wandell and Smirnakis 2009), and there are different ways to induce changes in the topographic organization of the cortex. Studies in primates have shown changes in the cortical structure by learning in somatosensory (Recanzone et al. 1992) and auditory (Recanzone et al. 1993) cortices, increasing the population that responds to a stimulus. Similarly, several studies have reported plasticity effects in the visual cortex of mammals after training in a repetitive visual task, improving visual perception (Karmarkar and Dan 2006). Another way to induce topographic reorganization in the cortex is by manipulating sensory activity. In V1, the elegant work from Charles Gilbert's laboratory showed an increase of approximately 5° in the RF size, with changes in the RF spatial location of approximately 1° immediately after removing the sensorial input by a localized lesion in the retina (Gilbert and Wiesel 1992). RF displacement increased over time and became as large as 5° 2 months after retinal lesion. Furthermore, inactivation of cortical feedback from V2/V3 areas has been shown to induce changes in surround supression in V1 neurons of awake macaques, altering their RFs spatio-temporal properties (Nassi et al. 2013). Finally, lesions produced in the cortex itself also modify the cortical topography. Studies carried out in anesthetized cats (Eysel and Schweigart 1999) showed an increase in the RF size of V1 neurons surrounding a lesion induced by ibotenic acid. In the thalamus, Krupa et al. (1999) have reported in rats that blocking SI produces immediate changes in RF plasticity, unmasking novel responses and eliminating existing responses for the same neuron. Also in rats, Ghazanfar et al. (2001) have shown enlargements and reductions of RFs in the somatosensory thalamus during cortical inactivation, and it has been demonstrated that blocking cortical N-methyl-d-aspartate receptors induced a dramatic expansion of RFs in the ventroposterior thalamus (Ergenzinger et al. 1998). Furthermore, in the auditory system, Nelson et al. (2015) have described frequency tuning shifts (up to 5 Khz) in MGBv neurons after electrical stimulation of the inferior colliculus in control conditions, but not when auditory cortex was inactivated using muscimol. These results suggest the existence of dynamic sensory mechanisms regulating the interchange of information between cortex and thalamus able to re-shape the preexisting RFs. In our study, we used rTMS@0.7 Hz to decrease cortical activity in a focal area of V1. This magnetic stimulation protocol creates a temporal "virtual lesion" in the cortical surface. In this situation, the surrounding cortical areas assume the functionality of the lesioned area, as happens in the case of real lesions, reorganizing the RF topography. It is likely that this topographical reorganization is somehow transferred down to the LGN by cortical feedback and is able to induce changes in the retinotopic organization of LGN cells. Prior to our work, multiple studies had been done in anaesthetized animals addressing the contribution of visual cortex to LGN RF properties. Especially, relevant here is Baker and Malpeli (1977) because visual cortex inactivation was reversible (cooling), and carried out on unanesthetized (but paralyzed) monkeys. Effects obtained were relatively minor and, in any case, did not affect RF topography. However, the different animal preparation and the differences in visual stimulation protocols, (they used large, full field, stimuli) make it difficult to establish comparisons and may have masked any putative RF displacement.

The remarkable shifts in RF position seem unlikely to be artifact. The animal's head was fixed to the chair, avoiding possible movements. Eye positions were continuously monitored by an eye tracker system that ensures that the animal is fixating at the center of the screen before stimulus presentation. Our results could easily be explained if the rTMS induced a shift in position of the nonmonitored eye (i.e., induced a strabismus) and we recorded through the nonmonitored eye. However, this did not happen. Some of the observed spatial effects occurred in the monitored eye.

Second, we subsequently monitored both eyes during rTMS inactivation of visual cortex and observed no gaze shifts. Furthermore, we analyzed the spike waveforms of each neuron evoked by visual stimulation in each position of the visual space, and a gamma test was performed to confirm that we were recording the same neuron. Even if for some bizarre reason the recorded cell disappeared and was immediately substituted by an indistinguishable neuron, the RF should be overlapped. All of these arguments make us confident that there was an actual displacement on the cells' RFs.

These results were unexpected and surprising based on what we know about the monkey visual system. Parvocellular cells have a RF of about 1 ° within the central 10 °, nonetheless, our results indicate either the retinal ganglion axons have a much broader sampling distribution, or the dendrites of the LGN neurons are sampling more broadly. Furthermore, the classic view of the retino-thalamic connections in monkey (and cat) points to low convergence, and almost 1:1 connectivity between the retina and the LGN, seemingly excluding the possibility of latent connections (Mastronarde 1987; Michael 1988). This view was reinforced by more recent experiments recording simultaneously S potentials and LGN spikes (Lee et al. 1983; Sincich et al. 2007) indicating low convergence. However, it is important to notice that none of these studies can specifically discard the existence of silent retino-thalamic connections. All these experiments were done with intact visual cortex, and looking for the active inputs to the LGN cell at a particular moment; any silent synapse would not be evident.

The possibility of the existence of dormant connections has been suggested in other species. Recent experiments in cats and mice (Moore et al. 2011; Hammer et al. 2015) support that idea and suggest that "functionally silent, nonspecific retinal inputs can serve as a substrate for rapid plasticity in the adult." Therefore, a tempting hypothesis may be formulated grounded on the existence of a main input from the retina to the thalamus, that coexists with secondary inputs masked in control conditions that can be "wakened" in certain circumstances (Fig. 10). Whereas the scheme does not fit with anatomical data from monkey, it may turn out that the monkey is actually more similar to the cat where retinal axons can extend across several millimeter and could account for the size of "jumps" observed here (Alonso et al. 2006; Rathbun et al. 2016). Retinal inputs share the spotlight with the complex corticothalamic glutamatergic terminals targeting GABAergic interneurons, TRN neurons, dendrites of relay cells, and possibly terminals of retinal axons. This complexity is enhanced by the fact that the associated glutamatergic receptors can produce EPSPs or IPSPs, and the interneurons can produce disynaptic circuits to change sign and duration of influence. Then, following the cartoon shown in Figure 9, V1 can directly potentiate a given location in visual space (position 1) through corticofugal axons operating via metabotropic receptors (Lam and Sherman 2013) and, simultaneously, blocks afferents from position 2 due to presynaptic inhibition mediated by GABAergic interneurons (Chen and Regehr 2003).

(*A*) This cartoon illustrates a possible explanation for the observed effects. Each subgroup had a different RF location at the LGN, hence it receives cortical feedback from different cortical locations within V1, one deeper than the other. As the TMS coil was always applied at the same position, it is conceivable that cortical cells were affected differently by the magnetic field, which rendered different modulatory effects on the LGN cells. (*B*) A given LGN neuron receives input from retinal cells covering an area higher than the classical RF, but cortical inputs potentiate those at the RF center (position 1) and simultaneously block the influence from peripheral inputs. For simplicity, we only show the circuit for the recorded neuron. Green represents excitatory inputs, red represents inhibitory ones. Input strength is represented by color intensity. (*C*) Cortical TMS on V1 at the frequency and intensity used in this work causes cortical depression (represented in the cartoon as pale color). This releases inhibition on peripheral inputs. Simultaneously, surrounding cortical areas increase their activity which inhibits inputs from position 2. Notice that the red line from relay cell represents presynaptic inhibition exerted by the cortical cell over the retino-thalamic synapse through metabotropic Glu receptors (Lam and Sherman 2013).

During rTMS-induced cortical blockade, there is an immediate reorganization of the system; the affected area decreases its activity, releasing the inhibition affecting position 2. Simultaneously, there is an increment of activity in the periphery at cortical level which inhibits inputs from position 1. The whole process induces the RF shift. The cortical extension of the effect, plus the retinotopic relationships between cortex and LGN would determine the shift direction and magnitude.

There were 2 principal angular directions for RF displacements: $\vartheta 1 = (111.87 \pm 16.43)°$ (subgroup A) and $\vartheta 2 = (43.14 \pm 22.66)°$ (subgroup B) (see Fig. 9). Each subgroup has different eccentricities, and, is therefore driven from different locations in the LGN (Fig. 9*B*). This implies that these subgroups receive different feedback from different cortical locations (Fig. 10). Although the TMS coil was always placed at the same cortical coordinates, the intensity and orientation of the magnetic field affecting those cortical locations seems to have been different, changing the cortical activity in complex ways that could explain 2 different displacement directions. The precise mechanism implicated will be the object of future studies, but the fact that rTMS stimulation can differently affect different groups of cells depending upon their location in the visual cortex could also explain why some neurons showed RF shifts and other did not. Furthermore, it could be related to different subpopulations of layer 6 corticofugal neurons (Briggs et al. 2016) differentially affected by our manipulation.

Neurons whose RF's shifted after rTMS exhibit lower eccentricity values than those whose RF did not shift ($P < 0.01$, *t*-test), which would have a retinotopic representation in V1 innermost in the sulcus. In this case, the magnetic field would not be strong enough to affect the neurons or change the spatial properties of the LGN cells. Furthermore, we did not find any other distinctive aspect in those cells whose RF shifted versus those that did not in terms of firing rate, spike waveform, depth at the LGN, etc. However, taking into account the retinotopic relationship between visual cortex and thalamus a plausible possibility could involve an optimal alignment between TMS at V1 and the recording electrode at the LGN. Experiments to check for this possibility, would probably include tiny and focal blockades of a restricted area on V1, perhaps using pharmacological/optogenetic techniques, and recordings in the correspondent locus at the level of the LGN. In our hands and using a behaving primate, it is not possible.

The observed effects lasted hours, waiting up to 3 h failed to show a recovery. We would like to emphasize, however, that when we used the same coordinates for next day penetration (we recorded from the same spatial location) the position of the RF was similar to the initial one of the recording session of preceding day. This long lasting effect may be related to the rTMS protocol employed. Although a single session of repetitive TMS at of 1 Hz produces short-term changes, continuous application, day after day (sometimes twice a day), induces long lasting effects (Chen et al. 1997; Muellbacher et al. 2000; Nyffeler et al. 2006; Plewnia et al. 2007). Such enduring changes form the basis for TMS treatment in various mental illnesses such as depression or anxiety (O'Reardon et al. 2007; Diefenbach et al. 2016). It could be that the intrasession lack of recovery is just reflecting a cortical LTP-like effect that overcomes the recording period for a particular cell (up to 3 h). Interestingly, those cells that showed a reduction in response but not a RF shift, recovered their responsiveness about 30 min after rTMS. The simplest interpretation, following the hypothesis mentioned above (see Fig. 10), would be to assume that the strength of the effect observed in the LGN reflects the intensity of the cortical block produced by rTMS. It will depend on the retinotopic alignment, the geometry of the cortex and the relative location of affected corticofugal cells with respect to the coil, which will define the intensity of the magnetic field reaching those neurons. In some cases, the V1 blockade is just enough to reduce the descendant excitatory input to the LGN but without silencing it. In other cases, V1 suppression is stronger, blocks the cortical influence on the LGN neuron yielding a functional inactivation of its normal retinal drive. The influence of cortical downflow from beyond the rTMS block can allow the unmasking of other latent retinal drives. This explanation is speculative and needs further confirmation.

rTMS to V1

rTMS has been widely used for a number of years as a useful tool for modulating cortical activity. Based upon early evidence showing that trains of stimuli delivered to the motor cortex could produce either increased or decreased corticospinal excitability, rTMS has become an excellent procedure for testing and modulating neuronal excitability (Kobayashi and Pascual-Leone 2003). Previous work have shown that low-frequency rTMS, similar to the one used in this paper, produces a reduction of the cortical activity (Chen et al. 1997; De Labra et al. 2007; Ortuño et al. 2014) that lasts up to 15 min after the magnetic stimulation is finished. In addition, previous work from our laboratory in anaesthetized animals (cat and monkey) where low rTMS was applied to V1 showed a reduction in responsiveness of LGN cells (De Labra et al. 2007; Espinosa et al. 2011). In this study, we report that rTMS at 0.7 Hz generates a significant decrease of both basal and evoked responses in the 49.3% of LGN cells recorded. We trust that this decrement is due to reduction of the corticothalamic input provoked by the cortical inhibition due to magnetic stimulation. The magnetic field magnitude is inversely proportional to the distance ($B \propto 1/r$) (Biot and Savart 1821), so a direct effect on subcortical structures is very unlikely (Deng et al. 2013).

Furthermore, we found a significant increase in the latency of LGN cells after cortical blockade. This result fits well with previous work (Espinosa et al. 2011) performed in anesthetized cats that showed an increment of latency of approximately 1 ms, when a similar rTMS protocol was used. This change is smaller in magnitude than the one obtained here, which could be due to the experimental model used (awake primate vs. anesthetized cat). The increase in latency could be due to the decrease of excitability at the LGN induced by the decrease of a tonic cortical excitatory input. In other words, the result suggests that in physiological conditions, the cortex, by modulating the membrane potential of thalamic cells, is capable of generating a locus of increased activity in the thalamus, thus facilitating the transfer of information from specific areas of the visual space.

In summary, we have shown that acute removal of feedback from V1 to LGN using rTMS in the awake monkey effectively shifts the RFs of LGN neurons by an average of 4.5°. These results, unpredictable based on our current understanding of sensory systems, suggest the existence of latent sensory inputs from the periphery that are being selected by feedback connections. In fact, our results evidence that the cortical feedback has an astonishing potential for modulating thalamic responses, being able to change even the RF position in some conditions, and hence demonstrating that RFs are dynamic structures. We would like to suggest that in normal conditions, this sort of iterative and dynamic reshaping of RFs happens in a much more controlled way, reflecting top-down influences related to attention or to other feedback-mediated processes.

Supplementary Material
Supplementary material are available at Cerebral Cortex online.

Author contributions
J.C. and C.R. imagined the study, and designed the experiments. J.A. performed the experiments and the analysis of the data, all the authors collaborated in the recording sessions and in the discussion and interpretation of the data. J.A., J.C., and C.R. wrote the manuscript. J.C. and C.R. contributed equally to this work.

Notes
We would like to thank the anonymous reviewers for their insightful comments on the paper. *Conflict of Interest*: None declared.

References

Alonso J-M, Yeh C-I, Weng C, Stoelzel C. 2006. Retinogeniculate connections: a balancing act between connection specificity and receptive field diversity. Prog Brain Res. 154:3–13.

Andolina IM, Jones HE, Sillito AM. 2013. Effects of cortical feedback on the spatial properties of relay cells in the lateral geniculate nucleus. J Neurophysiol. 109:889–899.

Andolina IM, Jones HE, Wang W, Sillito AM. 2007. Corticothalamic feedback enhances stimulus response precision in the visual system. Proc Natl Acad Sci. 104:1685–1690.

Aydin-Abidin S, Moliadze V, Eysel UT, Funke K. 2006. Effects of repetitive TMS on visually evoked potentials and EEG in the anaesthetized cat: dependence on stimulus frequency and train duration. J Physiol. 574:443–455.

Baker FH, Malpeli JG. 1977. Effects of cryogenic blockade of visual cortex on the responses of lateral geniculate neurons in the monkey. Exp brain Res. 29:433–444.

Biot J-B, Savart F. 1821. Sur l'aimantation imprimée aux métaux par l'électricité en mouvement. J des Savans. 221–235.

Briggs F, Kiley CW, Callaway EM, Usrey WM. 2016. Morphological substrates for parallel streams of corticogeniculate feedback originating in both V1 and V2 of the macaque monkey. Neuron. 90:388–399.

Briggs F, Usrey WM. 2011. Corticogeniculate feedback and visual processing in the primate. J Physiol. 589:33–40.

Chen C, Regehr WG. 2003. Presynaptic modulation of the retinogeniculate synapse. J Neurosci. 23:3130–3135.

Chen R, Classen J, Gerloff C, Celnik P, Wassermann EM, Hallett M, Cohen LG. 1997. Depression of motor cortex excitability by low-frequency transcranial magnetic stimulation. Neurology. 48:1398–1403.

Cudeiro J, Sillito AM. 1996. Spatial frequency tuning of orientation-discontinuity-sensitive corticofugal feedback to the cat lateral geniculate nucleus. J Physiol. 490:481–492.

Cudeiro J, Sillito AM. 2006. Looking back: corticothalamic feedback and early visual processing. Trends Neurosci. 29:298–306.

Darian-Smith C, Gilbert CD. 1995. Topographic reorganization in the striate cortex of the adult cat and monkey is cortically mediated. J Neurosci. 15:1631–1647.

De Labra C, Rivadulla C, Grieve K, Mariño J, Espinosa N, Cudeiro J. 2007. Changes in visual responses in the feline dLGN: selective thalamic suppression induced by transcranial magnetic stimulation of V1. Cereb Cortex. 17:1376–1385.

Deng Z-D, Lisanby SH, Peterchev AV, Roth Y, Pell GS, Zangen A. 2013. Electric field depth–focality tradeoff in transcranial magnetic stimulation: simulation comparison of 50 coil designs. Brain Stimul. 6:14–15.

Diefenbach GJ, Bragdon LB, Zertuche L, Hyatt CJ, Hallion LS, Tolin DF, Goethe JW, Assaf M. 2016. Repetitive transcranial magnetic stimulation for generalised anxiety disorder: a pilot randomised, double-blind, sham-controlled trial. Br J Psychiatry. 209:222–228.

Ergenzinger ER, Glasier MM, Hahm JO, Pons TP. 1998. Cortically induced thalamic plasticity in the primate somatosensory system. Nat Neurosci. 1:226–229.

Erisir A, Van Horn SC, Sherman SM. 1997. Relative numbers of cortical and brainstem inputs to the lateral geniculate nucleus. Proc Natl Acad Sci USA. 94:1517–1520.

Espinosa N, Mariño J, De Labra C, Cudeiro J. 2011. Cortical modulation of the transient visual response at thalamic level: a TMS study. PLoS One. 6:e17041.

Eysel UT, Schweigart G. 1999. Increased receptive field size in the surround of chronic lesions in the adult cat visual cortex. Cereb Cortex. 9:101–109.

Freedman D, Diaconis P. 1981. On the histogram as a density estimator: L 2 theory. Probab theory Relat fields. 57:453–476.

Gangitano M, Valero-Cabré A, Tormos JM, Mottaghy FM, Romero JR, Pascual-Leone Á. 2002. Modulation of input–output curves by low and high frequency repetitive transcranial magnetic stimulation of the motor cortex. Clin Neurophysiol. 113:1249–1257.

Ghazanfar A, Krupa D, Nicolelis M. 2001. Role of cortical feedback in the receptive field structure and nonlinear response properties of somatosensory thalamic neurons. Exp Brain Res. 141:88–100.

Gilbert CD. 1998. Adult cortical dynamics. Physiol Rev. 78:467–485.

Gilbert CD, Wiesel TN. 1992. Receptive field dynamics in adult primary visual cortex. Nature. 356:150–152.

Guido W, Weyand T. 1995. Burst responses in thalamic relay cells of the awake behaving cat. J Neurophysiol. 74:1782–1786.

Hammer S, Monavarfeshani A, Lemon T, Su J, Fox MA. 2015. Multiple retinal axons converge onto relay cells in the adult mouse thalamus. Cell Rep. 12:1575–1583.

Ichida JM, Casagrande VA. 2002. Organization of the feedback pathway from striate cortex (V1) to the lateral geniculate nucleus (LGN) in the owl monkey (Aotus trivirgatus). J Comp Neurol. 454:272–283.

Jones HE, Andolina IM, Ahmed B, Shipp SD, Clements JTC, Grieve KL, Cudeiro J, Salt TE, Sillito AM. 2012. Differential feedback modulation of center and surround mechanisms in parvocellular cells in the visual thalamus. J Neurosci. 32:15946–15951.

Jones HE, Andolina IM, Shipp SD, Adams DL, Cudeiro J, Salt TE, Sillito AM. 2015. Figure-ground modulation in awake primate thalamus. Proc Natl Acad Sci USA. 112:7085–7090.

Kaas JH. 1997. Topographic maps are fundamental to sensory processing. Brain Res Bull. 44:107–112.

Kaplan E, Shapley R. 1984. The origin of the S (slow) potential in the mammalian lateral geniculate nucleus. Exp brain Res. 55:111–116.

Karmarkar UR, Dan Y. 2006. Experience-dependent plasticity in adult visual cortex. Neuron. 52:577–585.

Kobayashi M, Pascual-Leone A. 2003. Transcranial magnetic stimulation in neurology. Lancet Neurol. 2:145–156.

Krupa DJ, Ghazanfar AA, Nicolelis MAL. 1999. Immediate thalamic sensory plasticity depends on corticothalamic feedback. Proc Natl Acad Sci. 96:8200–8205.

Lam Y-W, Sherman SM. 2013. Activation of both Group I and Group II metabotropic glutamatergic receptors suppress retinogeniculate transmission. Neuroscience. 242:78–84.

Lee BB, Virsu V, Creutzfeldt OD. 1983. Linear signal transmission from prepotentials to cells in the macaque lateral geniculate nucleus. Exp brain Res. 52:50–56.

Low DA, Harms WB, Mutic S, Purdy JA. 1998. A technique for the quantitative evaluation of dose distributions. Med Phys. 25:656–661.

Lu SM, Guido W, Sherman SM. 1992. Effects of membrane voltage on receptive field properties of lateral geniculate neurons in the cat: contributions of the low-threshold Ca2+ conductance. J Neurophysiol. 68:2185–2198.

Maccabee PJ, Amassian VE, Cracco RQ, Cracco JB, Rudell AP, Eberle LP, Zemon V. 1990. Magnetic coil stimulation of human visual cortex: studies of perception. Electroencephalogr Clin Neurophysiol Suppl. 43:111–120.

Maeda F, Keenan JP, Tormos JM, Topka H, Pascual-Leone A. 2000. Modulation of corticospinal excitability by repetitive transcranial magnetic stimulation. Clin Neurophysiol. 111:800–805.

Marrocco RT, McClurkin JW, Young RA. 1982. Modulation of lateral geniculate nucleus cell responsiveness by visual activation of the corticogeniculate pathway. J Neurosci. 2:256–263.

Mastronarde DN. 1987. Two classes of single-input X-cells in cat lateral geniculate nucleus. II. Retinal inputs and the generation of receptive-field properties. J Neurophysiol. 57:381–413.

McAlonan K, Cavanaugh J, Wurtz RH. 2008. Guarding the gateway to cortex with attention in visual thalamus. Nature. 456:391–394.

Michael CR. 1988. Retinal afferent arborization patterns, dendritic field orientations, and the segregation of function in the lateral geniculate nucleus of the monkey. Proc Natl Acad Sci USA. 85:4914–4918.

Moore BD, Kiley CW, Sun C, Usrey WM. 2011. Rapid plasticity of visual responses in the adult lateral geniculate nucleus. Neuron. 71:812–819.

Muellbacher W, Ziemann U, Boroojerdi B, Hallett M. 2000. Effects of low-frequency transcranial magnetic stimulation on motor excitability and basic motor behavior. Clin Neurophysiol. 111:1002–1007.

Murphy PC, Sillito AM. 1987. Corticofugal feedback influences the generation of length tuning in the visual pathway. Nature. 329:727–729.

Nassi JJ, Lomber SG, Born RT. 2013. Corticocortical feedback contributes to surround suppression in V1 of the alert primate. J Neurosci. 33:8504–8517.

Nelson SL, Kong L, Liu X, Yan J. 2015. Auditory cortex directs the input-specific remodeling of thalamus. Hear Res. 328:1–7.

Nyffeler T, Wurtz P, Lüscher H-R, Hess CW, Senn W, Pflugshaupt T, von Wartburg R, Lüthi M, Müri RM. 2006. Repetitive TMS over the human oculomotor cortex: comparison of 1-Hz and theta burst stimulation. Neurosci Lett. 409:57–60.

O'Connor DH, Fukui MM, Pinsk MA, Kastner S. 2002. Attention modulates responses in the human lateral geniculate nucleus. Nat Neurosci. 5:1203–1209.

O'Reardon JP, Solvason HB, Janicak PG, Sampson S, Isenberg KE, Nahas Z, McDonald WM, Avery D, Fitzgerald PB, Loo C, et al. 2007. Efficacy and safety of transcranial magnetic stimulation in the acute treatment of major depression: a multisite randomized controlled trial. Biol Psychiatry. 62:1208–1216.

Ortuño T, Grieve KL, Cao R, Cudeiro J, Rivadulla C. 2014. Bursting thalamic responses in awake monkey contribute to visual detection and are modulated by corticofugal feedback. Front Behav Neurosci. 8:198.

Pape H-C, McCormick DA. 1995. Electrophysiological and pharmacological properties of interneurons in the cat dorsal lateral geniculate nucleus. Neuroscience. 68:1105–1125.

Plewnia C, Reimold M, Najib A, Brehm B, Reischl G, Plontke SK, Gerloff C. 2007. Dose-dependent attenuation of auditory phantom perception (tinnitus) by PET-guided repetitive transcranial magnetic stimulation. Hum Brain Mapp. 28:238–246.

Ramcharan EJ, Gnadt JW, Sherman SM. 2003. Single-unit recording in the lateral geniculate nucleus of the awake behaving monkey. Methods. 30:142–151.

Rathbun DL, Alitto HJ, Warland DK, Usrey WM. 2016. Stimulus contrast and retinogeniculate signal processing. Front Neural Circuits. 10:8.

Recanzone GH, Merzenich MM, Jenkins WM, Grajski KA, Dinse HR. 1992. Topographic reorganization of the hand representation in cortical area 3b owl monkeys trained in a frequency-discrimination task. J Neurophysiol. 67:1031–1056.

Recanzone GH, Schreiner CE, Merzenich MM. 1993. Plasticity in the frequency representation of primary auditory cortex following discrimination training in adult owl monkeys. J Neurosci. 13:87–103.

Rivadulla C, Martínez LM, Varela C, Cudeiro J. 2002. Completing the corticofugal loop: a visual role for the corticogeniculate type 1 metabotropic glutamate receptor. J Neurosci. 22:2956–2962.

Sherman SM. 2001. Tonic and burst firing: dual modes of thalamocortical relay. Trends Neurosci. 24:122–126.

Sillito AM, Cudeiro J, Jones HE. 2006. Always returning: feedback and sensory processing in visual cortex and thalamus. Trends Neurosci. 29:307–316.

Sillito AM, Cudeiro J, Murphy PC. 1993. Orientation sensitive elements in the corticofugal influence on centre-surround interactions in the dorsal lateral geniculate nucleus. Exp Brain Res. 93:6–16.

Sillito AM, Jones HE, Gerstein GL, West DC. 1994. Feature-linked synchronization of thalamic relay cell firing induced by feedback from the visual cortex. Nature. 369:479–482.

Sincich LC, Adams DL, Economides JR, Horton JC. 2007. Transmission of spike trains at the retinogeniculate synapse. J Neurosci. 27:2683–2692.

Tsumoto T, Creutzfeldt OD, Legendy CR. 1978. Functional organization of the corticofugal system from visual cortex to lateral geniculate nucleus in the cat. Exp Brain Res. 32:345–364.

Van Horn SC, Erisir A, Sherman SM. 2000. Relative distribution of synapses in the A-laminae of the lateral geniculate nucleus of the cat. J Comp Neurol. 416:509–520.

Vanduffel W. 2000. Attention-dependent suppression of metabolic activity in the early stages of the macaque visual system. Cereb Cortex. 10:109–126.

Przybyszewski AW, Gaska JP, Foote W, Pollen DA. 2000. Striatecortex increases contrast gain of macaque LGN neurons. Vis Neurosci. 17:485–494.

Wandell BA, Smirnakis SM. 2009. Plasticity and stability of visual field maps in adult primary visual cortex. Nat Rev Neurosci. 10:873–884.

Wang W, Andolina IM, Lu Y, Jones HE, Sillito AM. 2016. Focal gain control of thalamic visual receptive fields by layer 6 corticothalamic feedback. Cereb Cortex. https://doi.org/10.1093/cercor/bhw376.

Wörgötter F, Eyding D, Macklis JD, Funke K. 2002. The influence of the corticothalamic projection on responses in thalamus and cortex. Philos Trans R Soc London B Biol Sci. 357:1823–1834.

Wörgötter F, Nelle E, Li B, Funke K. 1998. The influence of corticofugal feedback on the temporal structure of visual responses of cat thalamic relay cells. J Physiol. 509:797–815.